DMD Fast Forward. Published on November 8, 2007 as DOI: 10.1124/dmd.107.018788
DMD Fast Forward. Published on November 8, 2007 as doi:10.1124/dmd.107.018788
This article has not been copyedited and formatted. The final version may differ from this version.

DMD#18788

Resveratrol Glucuronidation Exhibits Atypical Enzyme Kinetics in Various Protein Sources

Otito Frances Iwuchukwu and Swati Nagar

Department of Pharmaceutical Sciences, Temple University, Philadelphia PA 19140

Downloaded from dmd.aspetjournals.org at ASPET Journals on April 10, 2024

Copyright 2007 by the American Society for Pharmacology and Experimental Therapeutics.

DMD Fast Forward. Published on November 8, 2007 as DOI: 10.1124/dmd.107.018788
This article has not been copyedited and formatted. The final version may differ from this version.

Running Title: Atypical Enzyme Kinetic Profiles of Resveratrol Glucuronides

Corresponding author:

Dr Swati Nagar

Department of Pharmaceutical Sciences

Temple University School of Pharmacy

3307 North Broad Street

Philadelphia, PA 19140

Tel: 215-707-9110

Fax: 215-707- 3678

Email: swati.nagar@temple.edu

Text Pages – 17

Tables – 1

Figures – 5

References – 38

Abstract – 243 words

Introduction – 750 words

Discussion – 1566 words

Downloaded from dmd.aspetjournals.org at ASPET Journals on April 10, 2024

DMD Fast Forward. Published on November 8, 2007 as DOI: 10.1124/dmd.107.018788
This article has not been copyedited and formatted. The final version may differ from this version.

Abbreviations used

UGT, UDP-glucuronosyl transferases

UDPGA, Uridine diphospho glucuronic acid

R3G, Resveratrol 3-O glucuronide

R4'G, Resveratrol 4'-O glucuronide

RES, Resveratrol

CXZ, Chlorzoxazone

DMSO, Dimethyl sulfoxide

E-H, Eadie-Hofstee Plots

Downloaded from dmd.aspetjournals.org at ASPET Journals on April 10, 2024

DMD Fast Forward. Published on November 8, 2007 as DOI: 10.1124/dmd.107.018788
This article has not been copyedited and formatted. The final version may differ from this version.

Abstract

The dietary polyphenol *trans*-resveratrol is glucuronidated at the 3 and 4' positions to yield two major glucuronide conjugates – resveratrol-3-*O*-glucuronide (R3G) and resveratrol-4'-*O*-glucuronide (R4'G). The major enzymes catalyzing this conjugation reaction are members of the UGT1A family and include UGT1A1 and UGT1A9, with minor contributions by UGT1A10. The kinetics of resveratrol glucuronidation in these three UGT1A isoforms as well as in human liver and intestinal microsomes were characterized across a wide concentration range. Atypical kinetics was observed for resveratrol glucuronidation in all the protein sources studied. The V_{max} estimate per total protein for both glucuronides was higher in human intestinal microsomes compared with human liver microsomes (12.2 ± 0.34 vs 7.4 ± 0.25 nmol/min/mg for R3G and 8.9 ± 0.14 vs 0.45 ± 0.01 nmol/min/mg for R4'G). The kinetic profile for formation of R3G in both human liver and intestinal microsomes fit a substrate inhibition model while that for R4'G exhibited a biphasic kinetic profile in human liver microsomes and substrate inhibition in human intestinal microsomes. In recombinant human UGT supersomes, for both glucuronides, UGT1A9 exhibited higher activity than UGT1A1 while the lowest activity was observed with UGT1A10. The kinetic profile for R3G exhibited substrate inhibition for all three isoforms while that for R4'G differed, exhibiting substrate inhibition for UGT1A1 and UGT1A10 and Hill kinetics for UGT1A9. These results suggest that i*n vitro* kinetics of resveratrol glucuronidation at high concentrations cannot be ignored in predicting *in vivo* clearance upon high dose consumption of resveratrol.

Downloaded from dmd.aspetjournals.org at ASPET Journals on April 10, 2024

DMD Fast Forward. Published on November 8, 2007 as DOI: 10.1124/dmd.107.018788
This article has not been copyedited and formatted. The final version may differ from this version.

Resveratrol (*trans*-resveratrol, 3,5,4'-trihydroxy-*trans*-stilbene, (Fig. 1); (referred to hereafter as resveratrol) is a dietary antioxidant polyphenol of plant origin (Aumont et al., 2001). It is found in grapes, cranberries, peanuts and red wine and is thought to possess a variety of beneficial effects (Wang et al., 2002). The most important and widely studied of these include its cardioprotective (Renaud and de Lorgeril, 1992) and chemopreventive (Jang et al., 1997) effects. Other biological effects attributed to resveratrol include anti-inflammatory and strong antioxidant effects (Baur and Sinclair, 2006). Resveratrol has additionally been reported to interfere with multiple stages of carcinogenesis including initiation, promotion and progression, while its ability to inhibit platelet aggregation and increase the expression of endothelial and inducible nitric oxide synthase was reported to be responsible for its cardioprotective effects (Jang et al., 1997; Chan et al., 2000; Bhat et al., 2001). A recent study implicated resveratrol in the improvement of health and protection of mice on a high calorie diet, with potential impact on obesity studies in humans (Baur et al., 2006).

Resveratrol is known to be glucuronidated in the small intestine of rat (Kuhnle et al., 2000) as well as in both the human GI tract (Sabolovic et al., 2006) and liver (de Santi et al., 2000a). Resveratrol glucuronidation is mediated by a multigenic family of enzymes known as UDP-glucuronosyltransferases (UGTs) which catalyze the transfer of the glucuronic acid moiety from the co-substrate UDP-glucuronic acid (UDPGA) to the substrate, usually resulting in a metabolite with greater polarity and water solubility. Several UGT isoforms exist and their expression in both the human liver and GI tract as well as their distinct but sometimes overlapping substrate specificity are well documented (Burchell and Coughtrie,

Downloaded from dmd.aspetjournals.org at ASPET Journals on April 10, 2024

DMD Fast Forward. Published on November 8, 2007 as DOI: 10.1124/dmd.107.018788
This article has not been copyedited and formatted. The final version may differ from this version.

1989; Mackenzie et al., 1997; Tukey and Strassburg, 2000). Resveratrol glucuronidation in the human liver is both regioselective and stereospecific, producing two major metabolites – resveratrol 3-O glucuronide (R3G) and resveratrol 4'-O glucuronide (R4'G) (Aumont et al., 2001). The formation of the two conjugates has been reported to occur at different rates, with the R3G being preferentially glucuronidated in both *cis* and *trans* resveratrol isomers.

Despite the purported effects of resveratrol, *in vivo* pharmacokinetic studies in both rats and humans show that resveratrol given orally results in very low plasma concentrations due to poor bioavailability. Resveratrol upon an oral dose is almost completely conjugated to its glucuronide and sulfate metabolites, with the major sulfate metabolite for resveratrol reported to be resveratrol-3-sulfate. Although resveratrol sulfation is not the goal of this study, the contribution of sulfation to resveratrol metabolism and its limited bioavailability is critical (De Santi et al., 2000b). Significant systemic levels of the sulfate metabolite upon oral resveratrol doses have been reported (Walle et al., 2004; Boocock et al., 2007). This has inevitably led to the hypothesis that these glucuronide and sulfate metabolites could also elicit pharmacological effects (Soleas et al., 2001a; Marier et al., 2002; Walle et al., 2004). Although glucuronidation is commonly thought of as a detoxification mechanism, several examples of active and / or toxic glucuronides exist in the literature (Burchell and Coughtrie, 1989). The observation that *in vivo* concentrations of both resveratrol and its glucuronides do not correspond with those required to elicit chemopreventive effects *in vitro* suggests higher resveratrol dose requirement for therapeutic effects (Goldberg et al., 2003). A recent phase 1 dose escalation study on resveratrol measured *in vivo* levels in an attempt to confirm these reported observations (Boocock et al., 2007).

Downloaded from dmd.aspetjournals.org at ASPET Journals on April 10, 2024

DMD Fast Forward. Published on November 8, 2007 as DOI: 10.1124/dmd.107.018788
This article has not been copyedited and formatted. The final version may differ from this version.

Although resveratrol glucuronidation in human liver and intestinal microsomes as well as several recombinant UGT preparations has been studied at either single or low concentrations (Brill et al., 2006; Sabolovic et al., 2006), characterization across a greater concentration range is necessary in the light of the potentially high dose requirement discussed above. Also, evaluating the kinetics of resveratrol glucuronidation over a wide concentration range will aid in comparison of independent studies conducted under variable experimental conditions, notably the different resveratrol concentrations utilized for single concentration metabolite formation velocities (de Santi et al., 2000a; Brill et al., 2006) . This study aims at characterizing the *in vitro* metabolic profiles for the two major resveratrol glucuronides across relevant enzyme sources. These sources include human liver and intestinal microsomes as well as those UGT1A isoforms reported to be specific for *trans*-resveratrol and which are differentially expressed in either the human liver or intestine - UGT1A1, 1A9 and 1A10 (Aumont et al., 2001). To the best of our knowledge, this is the first comprehensive report of resveratrol glucuronidation kinetics over a wide concentration range.

Downloaded from dmd.aspetjournals.org at ASPET Journals on April 10, 2024

DMD Fast Forward. Published on November 8, 2007 as DOI: 10.1124/dmd.107.018788
This article has not been copyedited and formatted. The final version may differ from this version.

Materials and Methods

Chemicals and Reagents. Resveratrol (*trans*-resveratrol), the co-factor uridine-5'-diphosphoglucuronic acid (UDPGA), *β*-glucuronidase (lyophilized powder from *E.Coli*), dimethyl sulfoxide (DMSO), alamethicin, and chlorzoxazone were purchased from Sigma-Aldrich (St. Louis, MO, USA). All chemicals used to prepare buffers and other reagents were of analytical grade. Pooled human liver and intestinal microsomes as well as Supersomes™ expressing the recombinant human UGT1A1, 1A9 and 1A10 isozymes were obtained from Gentest™ BD Biosciences (Bedford, MA). The primary anti-UGT1A antibody (sc-25487) for western blot analysis was purchased from Santa Cruz Biotechnology Inc (Santa Cruz, CA), while the secondary horseradish peroxidase conjugated goat anti-rabbit antibody as well as all other materials for western blots were purchased from Bio-Rad laboratories (Hercules, CA). SuperSignal® West Pico chemiluminescent substrate was purchased from Pierce (Rockford, IL).

Resveratrol glucuronidation assays

Resveratrol glucuronidation activity was determined in pooled human liver and intestinal microsomes as well as various recombinant UGT1A isoforms. The conditions for linearity with respect to time and protein concentration were optimized in preliminary studies. The assays were linear with respect to the selected time points and microsomal protein concentrations for each enzyme source. The incubation mixture consisting of enzyme fractions (final concentration 1mg/ml protein), the substrate resveratrol dissolved in DMSO (final DMSO concentration 10%v/v), alamethicin (10 μg/ml), $MgCl_2$ (5mM final concentration) and made up to final incubation volume with Tris-HCl buffer (100mM, pH

Downloaded from dmd.aspetjournals.org at ASPET Journals on April 10, 2024

DMD Fast Forward. Published on November 8, 2007 as DOI: 10.1124/dmd.107.018788
This article has not been copyedited and formatted. The final version may differ from this version.

7.4 at 37˚C) was preincubated for 3 minutes in a shaking water bath at 37˚C. An appropriate volume of the cofactor UDPGA (final concentration 5mM) was then added to start the reaction. A final volume of 100µl was used during preliminary studies for assay optimization and then scaled down to 50µl in subsequent assays. Concentrations of *trans*-resveratrol in the incubation mixtures ranged from 0.005 – 5 mM. The tubes were incubated in a shaking water bath for 30 minutes at 37°C. The reaction was quenched with equal volumes of an ice cold solution of the internal standard chlorzoxazone (10mM) in methanol. Samples were centrifuged at 12,000 rpm for four minutes and the supernatant was directly injected onto the HPLC column for analysis. For each enzyme fraction, appropriate negative control experiments were performed under the same conditions but without either substrate or UDPGA. The presence of resveratrol *β*-D-glucuronides was confirmed by testing their susceptibility to hydrolysis by *β*-glucuronidase. For this purpose, *β*-glucuronidase from *E.Coli* (6µL, final concentration 150 units) dissolved in 100 mM Tris Hydrochloride buffer (pH 7.4) was added to 50µL of the incubation mixture and incubated overnight at 37°C. The *β*-glucuronidase - treated mixture was subsequently quenched by the addition of an equal volume of an ice cold methanolic solution of chlorzoxazone (100mM). After precipitation of the proteins by centrifugation, the supernatant was then analyzed by HPLC. Control assays without *β*-glucuronidase were run under the same conditions, to estimate the stability of the glucuronide under the incubation conditions. All incubations were carried out in triplicate on two different occasions to afford a total of 6 replicates per assay.

Preliminary solubility studies indicated insolubility of resveratrol (1 – 5 mM final concentration) in aqueous solvents, even with 5% DMSO as a co-solvent. Therefore, all

Downloaded from dmd.aspetjournals.org at ASPET Journals on April 10, 2024

DMD Fast Forward. Published on November 8, 2007 as DOI: 10.1124/dmd.107.018788
This article has not been copyedited and formatted. The final version may differ from this version.

incubations were conducted with resveratrol dissolved in DMSO to yield a final high DMSO concentration of 10%. The effect of DMSO on the glucuronidation of resveratrol was therefore studied using three different concentrations of DMSO (2, 5 and 10% DMSO) and a substrate concentration range of 5-1000 uM. The effect of the higher DMSO concentrations on R3G formation was minor, differing only at the 500 uM concentration. However, R4'G formation at 500 and 1000 uM resveratrol was decreased significantly with 10% DMSO compared to 2% DMSO.

HPLC analysis

Pooled human liver and intestinal microsomes and the purified recombinant UGT1A proteins were characterized for catalytic activity toward the substrate resveratrol by a sensitive reverse phase HPLC assay using methods modified from those described by He and Aumont (Aumont et al., 2001; He et al., 2006). The HPLC system (HP 1100 series) consisted of a solvent delivery quaternary pump, an auto sampler with an injection valve fitted with a 200µl injection loop, a diode array detector with UV detection set at λ = 303nm, and a Zorbax SB C18 column (4.6 X 150mm, 5 µm particle size, Agilent Tech. Santa Clara, CA, USA). Integration was carried out using the software ChemStation version for LC Rev.A.08.01. The isocratic mobile phase consisted of 68.5% water and 31.5% buffer (Methanol/Glacial acetic acid 0.5%v/v) at a flow rate of 1ml min^{-1}. Analysis was carried out at ambient temperature. The areas of the glucuronide peaks formed were normalized to that of the internal standard (IS) chlorzoxazone. As pure standards of the resveratrol glucuronides were not commercially available, quantification of any resveratrol glucuronide(s) was performed by comparing the normalized peak areas to that of an external standard curve consisting of the parent

Downloaded from dmd.aspetjournals.org at ASPET Journals on April 10, 2024

DMD Fast Forward. Published on November 8, 2007 as DOI: 10.1124/dmd.107.018788
This article has not been copyedited and formatted. The final version may differ from this version.

compound resveratrol. The standard curve correlation coefficients were ≥ 0.99 and the validated assay exhibited intra and inter day coefficients of variation and bias of less than 10% for the concentration range studied.

Data analysis for enzyme kinetics

Prior to non-linear regression analysis, all data were transformed and Eadie-Hofstee curves plotted. The Michaelis-Menten model was fit only to data exhibiting linear Eadie-Hofstee plots in order to obtain kinetic parameter estimates. To determine Michaelis-Menten parameter estimates, the following equation was used to fit the data exhibiting linear Eadie-Hofstee plots:

$$v = V_{max}.[S]/ (K_m + [S]) \quad (1)$$

where v is the rate of the reaction, V_{max} is the maximum velocity estimate, [S] is the substrate concentration, and K_m is the Michaelis-Menten constant.

The following equations were used to fit the data exhibiting non linear Eadie-Hofstee plots:

a) for those exhibiting a partial substrate inhibition profile (Zhang et al., 1998),

$$v = V_1 (1+ (V_2.[S]/V_1.K_i))/ (1+ (Km/[S]) + ([S]/K_i)) \quad (2)$$

where K_i is the substrate inhibition constant

b) for those exhibiting a biphasic metabolism profile (Bowalgaha et al., 2005) ,

$$v = V_{max1}.[S]/ (K_1+[S]) + (V_{max2}.[S]/ (K_2+[S])) \quad (3)$$

where K_1 and K_2 represent the affinity constants for the two metabolic phases.

c) for those exhibiting a sigmoidal or autoactivation profile (Uchaipichat et al., 2004),

$$v = V_{max}.S^n/S_{50}{}^n + S^n \quad (4)$$

Downloaded from dmd.aspetjournals.org at ASPET Journals on April 10, 2024

DMD Fast Forward. Published on November 8, 2007 as DOI: 10.1124/dmd.107.018788
This article has not been copyedited and formatted. The final version may differ from this version.

where S_{50} is the substrate concentration resulting in 50% of V_{max} (analogous to K_m in previous equations) and *n* is the Hill coefficient. Nonlinear regression was performed with GraphPad Prism for Windows (version 4.03; GraphPad Software Inc., San Diego, CA). Statistical comparison of the parameter estimates was performed with GraphPad Instat using a two-sided t test assuming normal distribution, for which a p value < 0.01 was considered significant (Nagar et al., 2004).

Western blot analysis

UGT1A1 and UGT1A9 supersomes were subjected to western blot analysis for determination of relative levels of expressed UGT protein. Varying amounts (0.5 – 10 ug) of UGT1A1 and UGT1A9 supersomes (and 15 – 30 ug HLM as positive control) were electrophoresed on PAGEgel™ 10% SDS-polyacrylamide gels at 150 V for 1 h, and transferred on nitrocellulose membranes. The membrane was blocked in 5% milk in Tris – buffered saline with 0.05% Tween-20 (TTBS) for 1 h. This was followed by incubation with 1: 2000 anti-UGT1A primary antibody for 1 h. Membranes were washed for 30 min with TTBS, followed by incubation with 1: 1000 horseradish peroxidase conjugated anti-rabbit secondary antibody for 1 h. Membranes were washed with TTBS and incubated in SuperSignal® West Pico chemiluminescent substrate for 1 min. Upon exposing and developing the film, images were analyzed with the software ImageJ 1.38x (NIH USA) for densitometric measurements.

Downloaded from dmd.aspetjournals.org at ASPET Journals on April 10, 2024

DMD Fast Forward. Published on November 8, 2007 as DOI: 10.1124/dmd.107.018788
This article has not been copyedited and formatted. The final version may differ from this version.

Results

The glucuronidation of resveratrol was studied in five different protein sources to determine enzyme kinetic profiles for the formation of the two main glucuronide conjugates- resveratrol 3-O glucuronide (R3G) and resveratrol 4'-O glucuronide (R4'G) within a substrate concentration range of 5-5000 uM. (Fig. 1A) depicts the chemical structure of resveratrol showing the reported positions for resveratrol glucuronidation and the major and minor UGT 1A isoforms that catalyze conjugation at those positions (Aumont et al., 2001). A sample chromatogram from our assays showing retention times for the glucuronide products, the parent resveratrol and the internal standard chlorzoxazone is also depicted (Fig. 1B). R4'G, being the more polar metabolite, eluted before R3G (retention times were approximately 3 and 4 minutes respectively) (Aumont et al., 2001; Yu et al., 2002; Vitaglione et al., 2005; Brill et al., 2006).

In Fig. 2, the kinetic profiles for the formation of R3G in human liver microsomes (HLM), human intestinal microsomes (HIM), recombinant UGT1A1 supersomes and recombinant UGT1A9 supersomes are depicted with their Eadie- Hofstee (E-H) plots shown as insets. The corresponding enzyme kinetic parameters are listed in (Table 1). The R3G profiles exhibited substrate inhibition in all the enzyme systems. This was determined by fitting the data obtained to the substrate inhibition equation as specified under materials and methods to obtain correlation coefficients (r^2), the least sum of squares (SS) values, and by direct visualization of the E-H plots. The E-H plots for R3G formation exhibited a hook in the upper quadrant indicative of substrate inhibition kinetic profiles (Fig. 2 insets) (Hutzler and Tracy, 2002).

Downloaded from dmd.aspetjournals.org at ASPET Journals on April 10, 2024

DMD Fast Forward. Published on November 8, 2007 as DOI: 10.1124/dmd.107.018788
This article has not been copyedited and formatted. The final version may differ from this version.

Formation of R3G as evident by the V_{max} estimate per total protein was greatest in HIM, this rate being between 1.5 – 3 fold greater than that in HLM, UGT1A9 or 1A1. The K_m estimate for HIM (505.4 ± 29.4 μM) was significantly greater than that for HLM (280.4 ± 21.6 uM) with $p < 0.01$. The K_i estimates for this reaction were markedly different in HLM versus HIM (1022 ± 71.5 μM and 600.8 ± 20.5 μM for HLM and HIM respectively). The K_m and K_i estimates differed significantly between UGT1A1 and 1A9 (Table 1).

The kinetic profiles for the formation of R4'G in HLM, HIM, UGT1A1 and 1A9 are depicted in Fig. 3 along with their respective E-H plots shown as insets. The corresponding enzyme kinetic parameter estimates are listed (Table 1). In the case of R4'G, the kinetic profiles were different across the enzyme sources, exhibiting a substrate inhibition profile in HIM and UGT1A1, a biphasic metabolic profile in HLM and a sigmoidal (Hill kinetic) profile in UGT1A9. As with R3G formation, the best fits and kinetic profiles were determined by fitting data to the respective equations for the models, obtaining r^2 and least SS values and by visualization of the E-H plots. The E-H plots for HIM and UGT1A1 were also hook shaped (indicative of substrate inhibition profiles) while the E-H plot for HLM clearly showed a biphasic profile. The E-H plot for 1A9 was also characteristic of an enzyme exhibiting sigmoidal or autoactivation kinetics (Hutzler and Tracy, 2002). Interestingly, model fitting of the data obtained for UGT1A9 to the Michaelis-Menten equation provided similar goodness of fit estimates (data not shown). The maximal rate of formation of R4'G per total protein was highest in HIM; this rate was 4 and 10 fold greater when compared with 1A1 and 1A9 respectively. A direct comparison could not be made with HLM due to the biphasic kinetic

Downloaded from dmd.aspetjournals.org at ASPET Journals on April 10, 2024

DMD Fast Forward. Published on November 8, 2007 as DOI: 10.1124/dmd.107.018788
This article has not been copyedited and formatted. The final version may differ from this version.

profile obtained via HLM. The kinetics for formation of R4'G in UGT1A9 was best fit to the Hill equation with a Hill coefficient n = 1.6.

UGT expression levels in UGT1A1 and UGT1A9 supersome batches utilized in this study were compared with western blot analysis using the anti-UGT1A antibody. It was assumed that this antibody would exhibit similar affinity to both UGT1A isoforms. As shown in figure 4, at the amounts of total protein loaded (0.5 – 10 ug), UGT1A1 supersomes exhibited markedly higher levels of protein compared to UGT1A9. Based on these results, high reaction velocities catalyzed *via* UGT1A9 versus UGT1A1 are even greater when normalized by expressed UGT1A protein levels.

Figure 5 depicts the formation of R3G and R4'G in UGT1A10. Glucuronide formation is expressed as the normalized peak areas obtained from the peak area ratios of glucuronides to the internal standard over the concentration range studied. The formation of both glucuronides was very low and kinetic parameter estimates could not be obtained. However, visual observation of the plots indicated that both R3G and R4'G formation was inhibited at high substrate concentrations.

Overall the rate of formation of R3G per total protein was higher than that for R4'G in HLM and HIM, as well as recombinant UGT1A1 and UGT1A9. In UGT1A10 the maximum formation of R4'G seems greater if one considers only the formation peak area of the glucuronides as depicted. The rate of formation of both glucuronides was seen to be much higher in HIM than in any other protein source. Our data correlates well with previously

Downloaded from dmd.aspetjournals.org at ASPET Journals on April 10, 2024

DMD Fast Forward. Published on November 8, 2007 as DOI: 10.1124/dmd.107.018788
This article has not been copyedited and formatted. The final version may differ from this version.

published data regarding formation of resveratrol glucuronides in these enzyme systems (Aumont et al., 2001; Brill et al., 2006; Sabolovic et al., 2006). However, we observed an overall higher rate of UGT1A9 – catalyzed formation of R3G over R4'G within the substrate concentration range studied, which is in contrast to previously published reports (Aumont et al., 2001; Brill et al., 2006; Sabolovic et al., 2006).

Downloaded from dmd.aspetjournals.org at ASPET Journals on April 10, 2024

DMD Fast Forward. Published on November 8, 2007 as DOI: 10.1124/dmd.107.018788
This article has not been copyedited and formatted. The final version may differ from this version.

Discussion

Resveratrol is a dietary polyphenol with anticarcinogenic and cardioprotective effects, whose phase II conjugation by glucuronidation and sulfation in rats (Marier et al., 2002; Yu et al., 2002; Wenzel and Somoza, 2005), humans (de Santi et al., 2000a; De Santi et al., 2000b; Walle et al., 2004), various *in vitro* systems and recombinant enzyme preparations (Aumont et al., 2001; Kaldas et al., 2003; Brill et al., 2006; Sabolovic et al., 2006) has been evaluated. Studies were carried out with low substrate doses or concentration(s) ranging from 10nM to 1mM, assumed to be within acceptable limits for pharmacological activity. In studies with low dose resveratrol in rats (43ug/kg to 50mg/kg dose ranges) and humans (25mg oral dose), very low concentrations of resveratrol were found in plasma after either oral, i.p and i.v administration, but with measurable levels of various conjugated metabolites (Soleas et al., 2001a; Soleas et al., 2001b; Walle et al., 2004; Vitaglione et al., 2005; Wenzel and Somoza, 2005). This has led to the conclusions that a) the dose of resveratrol may have to be increased to produce measurable plasma levels and therefore therapeutic effects or b) resveratrol metabolites may possess pharmacological activity. In this study, we evaluated the glucuronidation kinetics of resveratrol *in vitro* across a wider concentration range than had been previously reported, to elucidate the impact of metabolism on its activity. The concept of administering very high doses of resveratrol for better therapeutic activity has been proposed and tested (Boocock et al., 2007).

The main UGT1A isoforms catalyzing the glucuronidation of *trans*-resveratrol are UGT1A1 and 1A9 (Aumont et al., 2001; Brill et al., 2006; Sabolovic et al., 2006). UGT1A1 is expressed in both the human liver and intestine while 1A9 is expressed only in the liver

Downloaded from dmd.aspetjournals.org at ASPET Journals on April 10, 2024

DMD Fast Forward. Published on November 8, 2007 as DOI: 10.1124/dmd.107.018788
This article has not been copyedited and formatted. The final version may differ from this version.

(Tukey and Strassburg, 2000; Nagar and Remmel, 2006). The putative intestine specific isoform UGT1A10 (Nagar and Remmel, 2006; Sabolovic et al., 2006) was also reported to be involved in resveratrol glucuronidation, although to a small extent (Aumont et al., 2001). Our results indicate that the kinetic profiles of the two main resveratrol conjugates (R3G and R4'G) in UGT1A1, 1A9 and HLM are markedly different. In HIM and UGT1A10, the profiles for both glucuronides were similar to one another, differing only in their rates of formation.

In HLM, substrate inhibition for R3G formation (table 1) was described by a two site model with one inhibitory binding site and the other operable at high substrate concentrations, resulting in decreased velocity with increasing concentrations (Shou et al., 2001; Hutzler and Tracy, 2002). De santi *et al* reported a K_m of 150 uM for overall resveratrol glucuronidation in HLM (de Santi et al., 2000a). The substrate concentration range used in that study (62.5 - 1000 uM) may explain why their data fit the Michaelis-Menten equation, had a lower K_m value and no inhibition was observed. These differences highlight the importance of characterizing enzyme kinetics across wider ranges of substrate concentration since the profiles at high concentrations may differ from those observed at lower less saturating concentrations.

For the formation of R4'G via HLM, the kinetics fit a biphasic model with a $V_{max2} > V_{max1}$ and a $K_{m2} >> K_{m1}$ where the velocity approaches V_{max2} at higher substrate concentrations without becoming asymptotic. Biphasic kinetics makes it difficult to predict or establish a single value for V_{max} and K_m (Korzekwa et al., 1998; Hutzler and Tracy, 2002). The biphasic

Downloaded from dmd.aspetjournals.org at ASPET Journals on April 10, 2024

DMD Fast Forward. Published on November 8, 2007 as DOI: 10.1124/dmd.107.018788
This article has not been copyedited and formatted. The final version may differ from this version.

profile obtained resembles that for a mixture of two different enzymes, one saturating at low concentrations and one with a very high Km (Korzekwa et al., 1998). It is not possible to determine which two isoforms within the HLM pool are responsible for the kinetics observed, but UGT1A1 and 1A9 are significant contributors based on their activities toward R4'G formation (table 1). With regard to rates of formation, even the highest velocity V_{max2} determined for R4'G was 6 fold less than that for R3G, consistent with previous reports (Aumont et al., 2001; Brill et al., 2006; Sabolovic et al., 2006).

In HIM the profiles for R3G and R4'G exhibit substrate inhibition, but the rate of formation for R3G was 1.5 fold greater than for R4'G, in agreement with previous reports (Brill et al., 2006; Sabolovic et al., 2006). This rate of formation obtained is per total protein concentration and not per individual UGT concentration. Lin *et al* have proposed the existence of two binding sites to explain substrate inhibition in CYP – mediated reactions (Lin et al., 2001; Shou et al., 2001). Although the mechanism of substrate inhibition may be unknown, ignoring atypical kinetics and truncating the data to fit Michaelis-Menten kinetics may lead to erroneous parameter estimates. The substrate inhibition profile obtained with HIM is similar to one with $V_{max2} < V_{max1}$ and a $K_{m2} = K_{m1}$ for a one enzyme two site model (Korzekwa et al., 1998). Assuming $K_i = K_{m2}$, we see that our data does indeed fit this model (table 1). Based on our results in HIM, the UGT1A isoform(s) responsible for glucuronidation of resveratrol would exhibit substrate inhibition. UGT 1A1, a major isoform for resveratrol glucuronidation in the liver (Aumont et al., 2001) has also been implicated in its intestinal metabolism (Brill et al., 2006; Sabolovic et al., 2006); this isozyme does indeed exhibit substrate inhibition kinetics for both glucuronides. Although it was reported not to

Downloaded from dmd.aspetjournals.org at ASPET Journals on April 10, 2024

DMD Fast Forward. Published on November 8, 2007 as DOI: 10.1124/dmd.107.018788
This article has not been copyedited and formatted. The final version may differ from this version.

contribute significantly to the formation of R4'G, its role in glucuronidation within the intestine cannot be ignored at such high concentrations, The putative intestine specific UGT1A10 also showed inhibition for both glucuronides although its contribution was very low. The formation rate reported for resveratrol glucuronidation in HIM is not adequately explained by the rates obtained with the individual recombinant UGTs utilized, and additional intestinal UGTs may therefore contribute. It is noteworthy that direct comparisons cannot be made between tissue microsomes and recombinant UGTs, due to obvious differences in these UGT sources (Miners et al., 2006).

For UGT1A1, the substrate inhibition profiles for R3G and R4'G fit a one enzyme two site model. This isozyme contributes significantly to the formation of R3G, as seen in its rate of formation. Brill *et al* (2006) reported a Km of 149 uM for R3G formation in UGT1A1 compared with 279 uM in this report, although the concentration range of resveratrol used was not stated. They also report that their data fit a Hill equation, which differs from our observations. With respect to the kinetics of R4'G, UGT1A1 seems to be a high affinity, low capacity isoform. The relevance of the relatively minor contribution of this isoform to the formation of R4'G remains to be seen.

With UGT1A9 supersomes, the substrate inhibition profile seen for R3G differs from that observed for UGT1A1 and HIM in that the apparent K_i and K_m values differ significantly. The rates of formation for R3G via UGT1A9 and UGT1A1 were equivalent. Previously published data (Aumont et al., 2001; Brill et al., 2006) state that among the UGT1A isoforms the highest rate of R3G formation is seen with UGT1A1, while we report the highest rate

Downloaded from dmd.aspetjournals.org at ASPET Journals on April 10, 2024

DMD Fast Forward. Published on November 8, 2007 as DOI: 10.1124/dmd.107.018788
This article has not been copyedited and formatted. The final version may differ from this version.

with UGT1A9, in agreement with Sabolovic *et al* (2006). The formation of R4'G in UGT1A9 exhibited Hill kinetics (suggesting autoactivation), also reported by Brill *et al* (2006). Hill kinetics have been previously reported for phase II metabolism (Fisher et al., 2000).

It is important to perform these experiment after eliminating artifactual sources of atypical kinetics (Hutzler and Tracy, 2002). Such sources include significant substrate depletion, low substrate solubility, paucity of data points, lack of analytical sensitivity and use of multi-enzyme systems (Houston and Kenworthy, 2000). We have taken care to exclude most of the sources cited. The very low solubility of resveratrol and the higher concentrations studied led to the high final DMSO concentration used. High concentrations of organic solvents may lead to substrate inhibition. With the exception of UGT 1A6, 2B15, and 2B17, organic solvent concentrations of 0.5 and 1% are reported to have minor though variable effects on isoform activity (Uchaipichat et al., 2004). While the concentration of DMSO used in this study may have decreased the R4'G formation, we note here that this effect was not inhibitory; the profile for R4'G in HLM was seen to be biphasic, while exhibiting a sigmoidal profile in UGT1A9 (Fig. 1A and 1D).

Having characterized the *in vitro* atypical kinetics of resveratrol glucuronidation, the question remains as to whether similar kinetics will be observed *in vivo* (Hutzler and Tracy, 2002). Even in the absence of atypical kinetics *in vivo*, complex *in vitro* kinetics may affect how data is scaled to the *in vivo* situation, because atypical kinetics may not allow for the simple use of the intrinsic clearance (CL_{int}) obtained by dividing the V_{max}/K_m as in the case of

Downloaded from dmd.aspetjournals.org at ASPET Journals on April 10, 2024

DMD Fast Forward. Published on November 8, 2007 as DOI: 10.1124/dmd.107.018788
This article has not been copyedited and formatted. The final version may differ from this version.

hyperbolic kinetics. The estimation of intrinsic clearance from atypical kinetics has been described (Venkatakrishnan et al., 2001) but assumed that the substrate concentration is well below the Km, a situation which does not apply in this study.

In conclusion, the glucuronidation of resveratrol studied in a variety of protein sources showed that rate of glucuronidation varied between the two main resveratrol glucuronides across the various enzyme sources. The formation of R3G was higher that of R4'G in all the enzyme sources; glucuronide formation was very low via recombinant UGT1A10. The atypical kinetics observed with resveratrol glucuronidation at this wide concentration range cannot be ignored, and may prove useful in predicting *in vivo* clearance upon consumption of very high doses of resveratrol.

Downloaded from dmd.aspetjournals.org at ASPET Journals on April 10, 2024

DMD Fast Forward. Published on November 8, 2007 as DOI: 10.1124/dmd.107.018788
This article has not been copyedited and formatted. The final version may differ from this version.

Acknowledgments

The authors wish to thank Miss Din Ung (Department of Pharmaceutical Sciences, Temple University) for her technical and administrative assistance.

Downloaded from dmd.aspetjournals.org at ASPET Journals on April 10, 2024

DMD Fast Forward. Published on November 8, 2007 as DOI: 10.1124/dmd.107.018788
This article has not been copyedited and formatted. The final version may differ from this version.

References

Aumont V, Krisa S, Battaglia E, Netter P, Richard T, Merillon JM, Magdalou J and Sabolovic N (2001) Regioselective and stereospecific glucuronidation of trans- and cis-resveratrol in human. *Arch Biochem Biophys* **393:**281-289.

Baur JA, Pearson KJ, Price NL, Jamieson HA, Lerin C, Kalra A, Prabhu VV, Allard JS, Lopez-Lluch G, Lewis K, Pistell PJ, Poosala S, Becker KG, Boss O, Gwinn D, Wang M, Ramaswamy S, Fishbein KW, Spencer RG, Lakatta EG, Le Couteur D, Shaw RJ, Navas P, Puigserver P, Ingram DK, de Cabo R and Sinclair DA (2006) Resveratrol improves health and survival of mice on a high-calorie diet. *Nature* **444:**337-342.

Baur JA and Sinclair DA (2006) Therapeutic potential of resveratrol: the in vivo evidence. *Nat Rev Drug Discov* **5:**493-506.

Bhat KPL, Kosmeder JW, 2nd and Pezzuto JM (2001) Biological effects of resveratrol. *Antioxid Redox Signal* **3:**1041-1064.

Boocock DJ, Faust GE, Patel KR, Schinas AM, Brown VA, Ducharme MP, Booth TD, Crowell JA, Perloff M, Gescher AJ, Steward WP and Brenner DE (2007) Phase I dose escalation pharmacokinetic study in healthy volunteers of resveratrol, a potential cancer chemopreventive agent. *Cancer Epidemiol Biomarkers Prev* **16:**1246-1252.

Bowalgaha K, Elliot DJ, Mackenzie PI, Knights KM, Swedmark S and Miners JO (2005) S-Naproxen and desmethylnaproxen glucuronidation by human liver microsomes and recombinant human UDP-glucuronosyltransferases (UGT): role of UGT2B7 in the elimination of naproxen. *Br J Clin Pharmacol* **60:**423-433.

Downloaded from dmd.aspetjournals.org at ASPET Journals on April 10, 2024

DMD Fast Forward. Published on November 8, 2007 as DOI: 10.1124/dmd.107.018788
This article has not been copyedited and formatted. The final version may differ from this version.

Brill SS, Furimsky AM, Ho MN, Furniss MJ, Li Y, Green AG, Bradford WW, Green CE, Kapetanovic IM and Iyer LV (2006) Glucuronidation of trans-resveratrol by human liver and intestinal microsomes and UGT isoforms. *J Pharm Pharmacol* **58:**469-479.

Burchell B and Coughtrie MWH (1989) UDP-glucuronosyltransferases. *Pharmacol Ther* **43:**261-289.

Chan MM, Mattiacci JA, Hwang HS, Shah A and Fong D (2000) Synergy between ethanol and grape polyphenols, quercetin, and resveratrol, in the inhibition of the inducible nitric oxide synthase pathway. *Biochem Pharmacol* **60:**1539-1548.

de Santi C, Pietrabissa A, Mosca F and Pacifici GM (2000a) Glucuronidation of resveratrol, a natural product present in grape and wine, in the human liver. *Xenobiotica* **30:**1047-1054.

De Santi C, Pietrabissa A, Spisni R, Mosca F and Pacifici GM (2000b) Sulphation of resveratrol, a natural compound present in wine, and its inhibition by natural flavonoids. *Xenobiotica* **30:**857-866.

Fisher MB, Campanale K, Ackermann BL, VandenBranden M and Wrighton SA (2000) In vitro glucuronidation using human liver microsomes and the pore-forming peptide alamethicin. *Drug Metab Dispos* **28:**560-566.

Goldberg DM, Yan J and Soleas GJ (2003) Absorption of three wine-related polyphenols in three different matrices by healthy subjects. *Clin Biochem* **36:**79-87.

He H, Chen X, Wang G, Wang J and Davey AK (2006) High-performance liquid chromatography spectrometric analysis of trans-resveratrol in rat plasma. *J Chromatogr B Analyt Technol Biomed Life Sci* **832:**177-180.

Downloaded from dmd.aspetjournals.org at ASPET Journals on April 10, 2024

DMD Fast Forward. Published on November 8, 2007 as DOI: 10.1124/dmd.107.018788
This article has not been copyedited and formatted. The final version may differ from this version.

Houston JB and Kenworthy KE (2000) In vitro-in vivo scaling of CYP kinetic data not consistent with the classical Michaelis-Menten model. *Drug Metab Dispos* **28:**246-254.

Hutzler JM and Tracy TS (2002) Atypical kinetic profiles in drug metabolism reactions. *Drug Metab Dispos* **30:**355-362.

Jang M, Cai L, Udeani GO, Slowing KV, Thomas CF, Beecher CW, Fong HH, Farnsworth NR, Kinghorn AD, Mehta RG, Moon RC and Pezzuto JM (1997) Cancer chemopreventive activity of resveratrol, a natural product derived from grapes. *Science* **275:**218-220.

Kaldas M, Walle U and Walle T (2003) Resveratrol transport and metabolism by human intestinal Caco-2 cells. *J Pharm Pharmacol* **55:**307 - 312.

Korzekwa KR, Krishnamachary N, Shou M, Ogai A, Parise RA, Rettie AE, Gonzalez FJ and Tracy TS (1998) Evaluation of atypical cytochrome P450 kinetics with two-substrate models: evidence that multiple substrates can simultaneously bind to cytochrome P450 active sites. *Biochemistry* **37:**4137-4147.

Kuhnle G, Spencer JP, Chowrimootoo G, Schroeter H, Debnam ES, Srai SK, Rice-Evans C and Hahn U (2000) Resveratrol is absorbed in the small intestine as resveratrol glucuronide. *Biochem Biophys Res Commun* **272:**212-217.

Lin Y, Lu P, Tang C, Mei Q, Sandig G, Rodrigues AD, Rushmore TH and Shou M (2001) Substrate inhibition kinetics for cytochrome P450-catalyzed reactions. *Drug Metab Dispos* **29:**368-374.

Mackenzie PI, Owens IS, Burchell B, Bock KW, Bairoch A, Belanger A, Fournel-Gigleux S, Green M, Hum DW, Iyanagi T, Lancet D, Louisot P, Magdalou J, Chowdhury JR,

Downloaded from dmd.aspetjournals.org at ASPET Journals on April 10, 2024

DMD Fast Forward. Published on November 8, 2007 as DOI: 10.1124/dmd.107.018788
This article has not been copyedited and formatted. The final version may differ from this version.

Ritter JK, Schachter H, Tephly TR, Tipton KF and Nebert DW (1997) The UDP glycosyltransferase gene superfamily: recommended nomenclature update based on evolutionary divergence. *Pharmacogenetics* **7:**255-269.

Marier JF, Vachon P, Gritsas A, Zhang J, Moreau JP and Ducharme MP (2002) Metabolism and disposition of resveratrol in rats: extent of absorption, glucuronidation, and enterohepatic recirculation evidenced by a linked-rat model. *J Pharmacol Exp Ther* **302:**369-373.

Miners JO, Knights KM, Houston JB and Mackenzie PI (2006) In vitro-in vivo correlation for drugs and other compounds eliminated by glucuronidation in humans: pitfalls and promises. *Biochem Pharmacol* **71:**1531-1539.

Nagar S, Remmel R, Hebbel R and Zimmerman C (2004) Metabolism of opioids is altered in liver microsomes of sickle cell transgenic mice. *Drug Metabolism and Disposition* **32:**98 - 104.

Nagar S and Remmel RP (2006) Uridine diphosphoglucuronosyltransferase pharmacogenetics and cancer. *Oncogene* **25:**1659-1672.

Renaud S and de Lorgeril M (1992) Wine, alcohol, platelets, and the French paradox for coronary heart disease. *Lancet* **339:**1523-1526.

Sabolovic N, Humbert AC, Radominska-Pandya A and Magdalou J (2006) Resveratrol is efficiently glucuronidated by UDP-glucuronosyltransferases in the human gastrointestinal tract and in Caco-2 cells. *Biopharm Drug Dispos* **27:**181-189.

Shou M, Lin Y, Lu P, Tang C, Mei Q, Cui D, Tang W, Ngui JS, Lin CC, Singh R, Wong BK, Yergey JA, Lin JH, Pearson PG, Baillie TA, Rodrigues AD and Rushmore TH (2001) Enzyme kinetics of cytochrome P450-mediated reactions. *Curr Drug Metab* **2:**17-36.

Downloaded from dmd.aspetjournals.org at ASPET Journals on April 10, 2024

DMD Fast Forward. Published on November 8, 2007 as DOI: 10.1124/dmd.107.018788
This article has not been copyedited and formatted. The final version may differ from this version.

Soleas GJ, Angelini M, Grass L, Diamandis EP and Goldberg DM (2001a) Absorption of trans-resveratrol in rats. *Methods Enzymol* **335:**145-154.

Soleas GJ, Yan J and Goldberg DM (2001b) Measurement of trans-resveratrol, (+)-catechin, and quercetin in rat and human blood and urine by gas chromatography with mass selective detection. *Methods Enzymol* **335:**130-145.

Tukey R and Strassburg C (2000) Human UDP-glucuronosyltransferases: metabolism, expression, and disease. *Annual Reviews in Pharmacology and Toxicology* **40:**581 - 616.

Uchaipichat V, Mackenzie PI, Guo XH, Gardner-Stephen D, Galetin A, Houston JB and Miners JO (2004) Human udp-glucuronosyltransferases: isoform selectivity and kinetics of 4-methylumbelliferone and 1-naphthol glucuronidation, effects of organic solvents, and inhibition by diclofenac and probenecid. *Drug Metab Dispos* **32:**413-423.

Venkatakrishnan K, Von Moltke LL and Greenblatt DJ (2001) Human drug metabolism and the cytochromes P450: application and relevance of in vitro models. *J Clin Pharmacol* **41:**1149-1179.

Vitaglione P, Sforza S, Galaverna G, Ghidini C, Caporaso N, Vescovi PP, Fogliano V and Marchelli R (2005) Bioavailability of trans-resveratrol from red wine in humans. *Mol Nutr Food Res* **49:**495-504.

Walle T, Hsieh F, DeLegge MH, Oatis JE, Jr. and Walle UK (2004) High absorption but very low bioavailability of oral resveratrol in humans. *Drug Metab Dispos* **32:**1377-1382.

Downloaded from dmd.aspetjournals.org at ASPET Journals on April 10, 2024

DMD Fast Forward. Published on November 8, 2007 as DOI: 10.1124/dmd.107.018788
This article has not been copyedited and formatted. The final version may differ from this version.

Wang Y, Catana F, Yang Y, Roderick R and van Breemen RB (2002) An LC-MS method for analyzing total resveratrol in grape juice, cranberry juice, and in wine. *J Agric Food Chem* **50:**431-435.

Wenzel E and Somoza V (2005) Metabolism and bioavailability of trans-resveratrol. *Mol Nutr Food Res* **49:**472-481.

Yu C, Shin YG, Chow A, Li Y, Kosmeder JW, Lee YS, Hirschelman WH, Pezzuto JM, Mehta RG and van Breemen RB (2002) Human, rat, and mouse metabolism of resveratrol. *Pharm Res* **19:**1907-1914.

Zhang H, Varlamova O, Vargas FM, Falany CN and Leyh TS (1998) Sulfuryl transfer: the catalytic mechanism of human estrogen sulfotransferase. *J Biol Chem* **273:**10888-10892.

Downloaded from dmd.aspetjournals.org at ASPET Journals on April 10, 2024

DMD Fast Forward. Published on November 8, 2007 as DOI: 10.1124/dmd.107.018788
This article has not been copyedited and formatted. The final version may differ from this version.

Footnotes

This work was partially supported by grants from the Cancer Research and Prevention Foundation, Alexandria VA, and Temple University Research Incentive Funds to SN.

This work has been accepted for presentation as a poster at the 2007 Annual meeting of the American Association of Pharmaceutical Scientists, to be held Nov 11 – 15 in San Diego CA.

Downloaded from dmd.aspetjournals.org at ASPET Journals on April 10, 2024

DMD Fast Forward. Published on November 8, 2007 as DOI: 10.1124/dmd.107.018788
This article has not been copyedited and formatted. The final version may differ from this version.

Figure Legends

Figure 1

(A) Chemical structure of *trans*-resveratrol and **(B)** a representative chromatogram showing the retention times for resveratrol (RES), resveratrol 3-O glucuronide (R3G), resveratrol 4'-O glucuronide (R4'G) and the internal standard chlorzoxazone (CXZ). The arrows on the chemical structure indicate the positions of the glucuronides formed and the reported major and minor UGT1A isoforms responsible for glucuronidation at those positions (Aumont et al., 2001). Major isoforms are indicated in bold letters.

Figure 2

Atypical kinetic profiles for formation of resveratrol 3-O Glucuronide (R3G) in A) Pooled human liver microsomes (HLM), B) Pooled human intestinal microsomes (HIM), C) Recombinant human UGT1A1, and D) Recombinant human UGT1A9 supersomes

Inset; The Eadie-Hofstee plots for each of the profiles are shown. Data reported as mean ± SEM, n = 6. Incubations were carried out across a 5 – 5000 μM substrate concentration range.

Figure 3

Atypical kinetic profiles for formation of resveratrol 4'-O Glucuronide (R4'G) in A) Pooled human liver microsomes (HLM), B) Pooled human intestinal microsomes (HIM), C) Recombinant human UGT1A1, and D) Recombinant human UGT1A9 supersomes

Downloaded from dmd.aspetjournals.org at ASPET Journals on April 10, 2024

DMD Fast Forward. Published on November 8, 2007 as DOI: 10.1124/dmd.107.018788
This article has not been copyedited and formatted. The final version may differ from this version.

Inset; The Eadie-Hofstee plots for each of the profiles are shown. Data reported as mean ± SEM, n = 6. Incubations were carried out across a 5 – 5000 μM Substrate concentration range.

Figure 4

Western blot analysis for the comparison of UGT1A expression in UGT1A1 and UGT1A9 supersomes. Varying amounts (0.5 – 10 ug total protein) of each supersome were loaded, with HLM (15 and 30 ug) as the positive control. Due to the low levels of UGT1A9 obtained upon an initial 30s exposure of film, the film was overexposed (1 min) to obtain measurable UGT1A9 bands. The data are additionally represented as a bar graph of total protein loaded (X-axis) versus optical density measured with ImageJ (Y-axis). Western blots were replicated on three separate occasions, and a representative blot is shown.

Figure 5

Atypical kinetic profiles seen in a plot of normalized glucuronide peak areas for formation of A) resveratrol 3-O glucuronide (R3G) and B) resveratrol 4'-O glucuronide (R4'G) in recombinant human UGT1A10 supersomes. Data reported as mean ± SEM, n = 6. Incubations were carried out across a 5 – 5000 μM substrate concentration range.

Downloaded from dmd.aspetjournals.org at ASPET Journals on April 10, 2024

DMD Fast Forward. Published on November 8, 2007 as DOI: 10.1124/dmd.107.018788
This article has not been copyedited and formatted. The final version may differ from this version.

Table 1: Kinetic parameter estimates for the glucuronidation of *trans*-resveratrol by Human liver and intestinal microsomes and recombinant UGT1A isoforms

Conjugation Product	Protein Source	V_{max}	K_m	K_i	Type of Fit	Goodness of Fit (r^2)
Resveratrol 3-O Glucuronide (R3G)	HLM	7.4 ± 0.25	280.4 ± 21.6	1022 ± 71.5	PSI	0.91
	HIM	12.2 ± 0.34	505.4 ± 29.4[a]	600.8 ± 20.5[a]	PSI	0.95
	UGT1A1	4.4 ± 0.22	279 ± 20.53	383 ± 5.4	PSI	0.93
	UGT1A9	5.4 ± 0.13	109.5 ± 5.9 [b]	613.5 ± 18.9[b,c]	PSI	0.94
Resveratrol 4'-O Glucuronide (R4'G)	HLM	V_{max1} = 0.45 ± 0.01 V_{max2} = 1.3 ± 0.03	K_{m1} = 65.2 ± 29 K_{m2} = 1685 ± 106.8	na	BPM	0.96
	HIM	8.9 ± 0.14	454.5 ± 21.8	564.3 ± 38.1	PSI	0.95
	UGT1A1	0.86 ± 0.02	50.7 ± 1.9	129.7 ± 2.8	PSI	0.97
	UGT1A9	2.2 ± 0.05	750	na	Hill (n=1.6)	0.95

Data are expressed as estimate ± SE, n = 6. Estimate units are as follows: Vmax, V_2 = nmol/min/mg; K_m, K_i = uM. PSI = Partial Substrate Inhibition, BPM = Biphasic Metabolism, HLM = Human liver microsomes, HIM = Human intestinal microsomes, na = not applicable.

a: HLM versus HIM estimate significantly different, $p < 0.01$. b: UGT1A1 versus UGT1A9 estimate significantly different, $p < 0.01$. c: K_i was significantly greater than the Km for R3G formation in UGT1A9, $p < 0.01$

Downloaded from dmd.aspetjournals.org at ASPET Journals on April 10, 2024

Figure 1

DMD Fast Forward. Published on November 8, 2007 as DOI: 10.1124/dmd.107.018788
This article has not been copyedited and formatted. The final version may differ from this version.

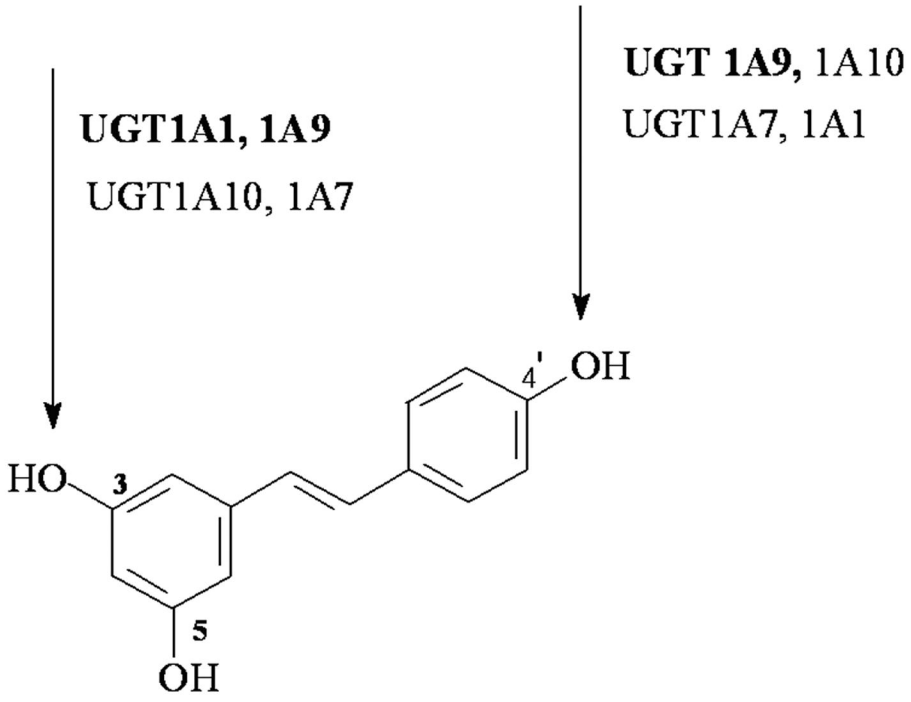

***trans*- resveratrol**

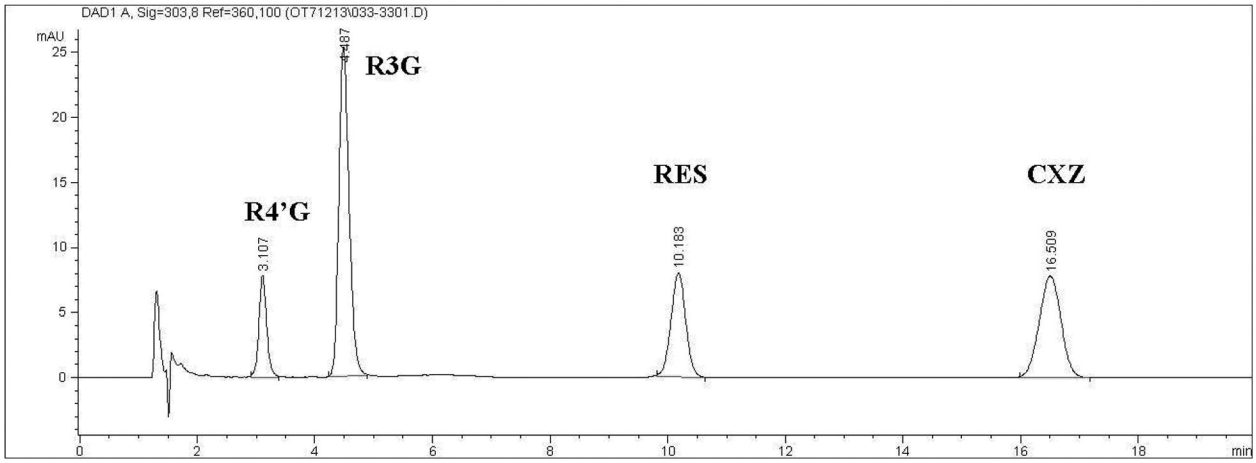

Downloaded from dmd.aspetjournals.org at ASPET Journals on April 10, 2024

DMD Fast Forward. Published on November 8, 2007 as DOI: 10.1124/dmd.107.018788
This article has not been copyedited and formatted. The final version may differ from this version.

Figure 2

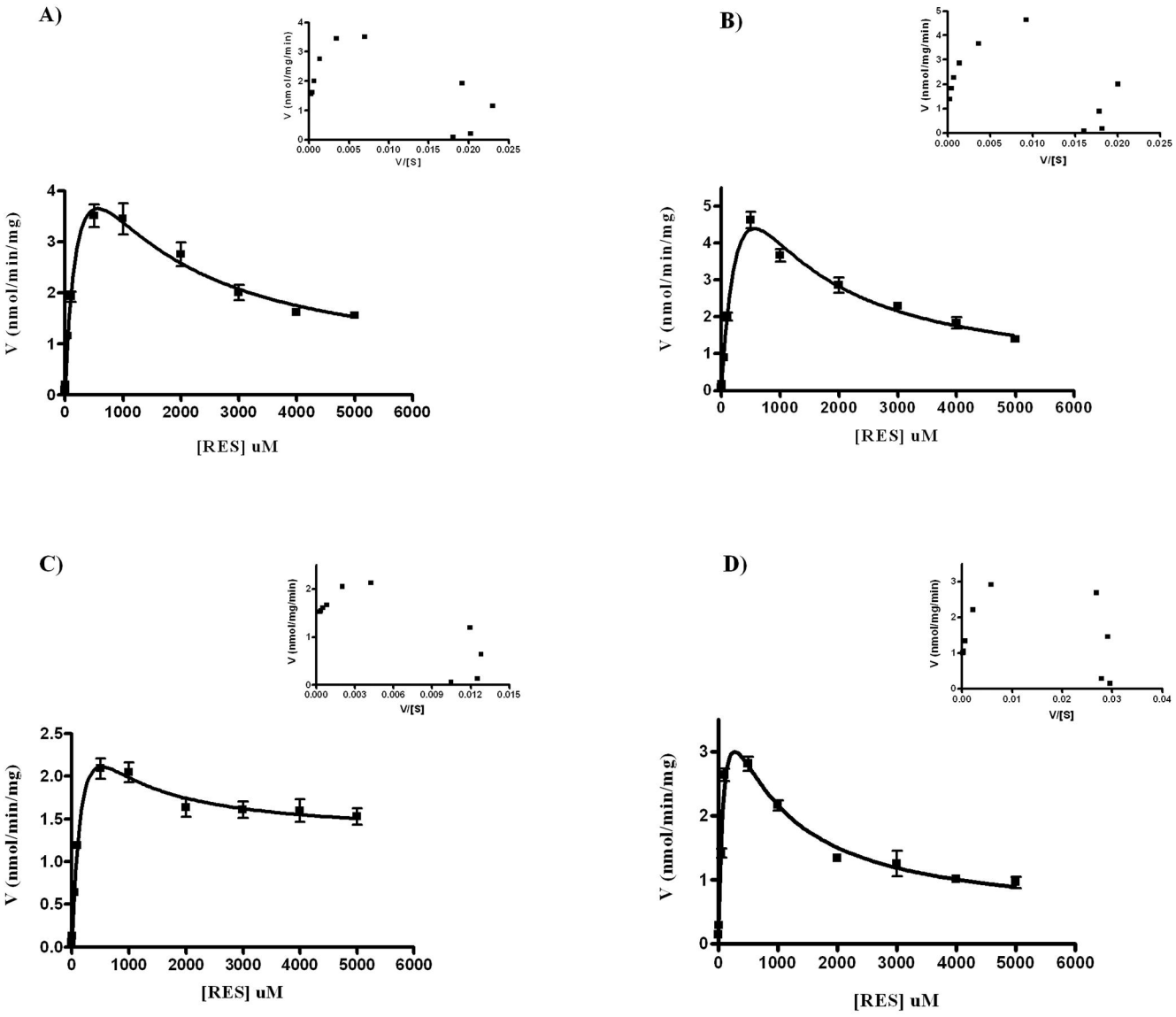

Downloaded from dmd.aspetjournals.org at ASPET Journals on April 10, 2024

DMD Fast Forward. Published on November 8, 2007 as DOI: 10.1124/dmd.107.018788
This article has not been copyedited and formatted. The final version may differ from this version.

Figure 3

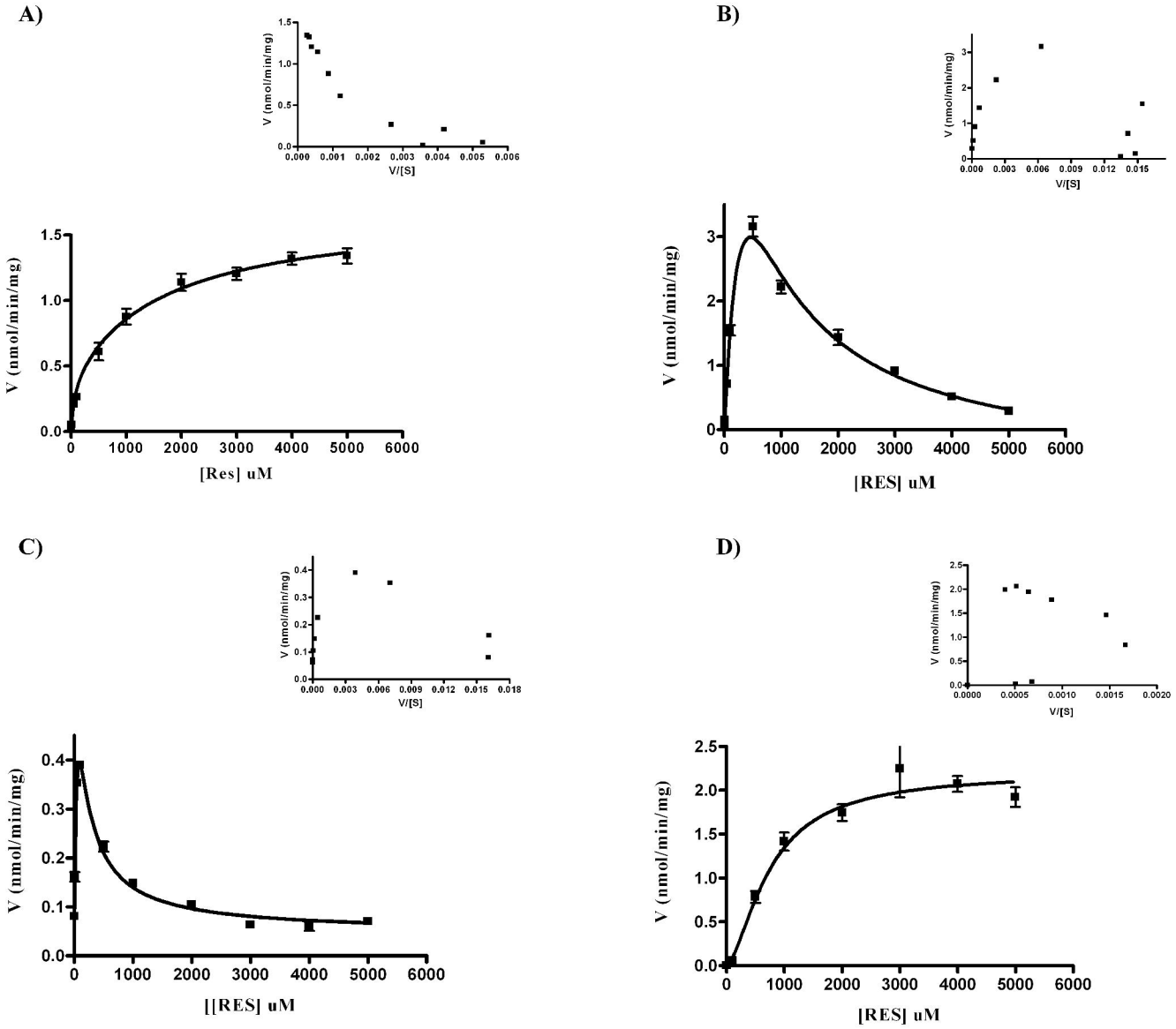

Downloaded from dmd.aspetjournals.org at ASPET Journals on April 10, 2024

DMD Fast Forward. Published on November 8, 2007 as DOI: 10.1124/dmd.107.018788
This article has not been copyedited and formatted. The final version may differ from this version.

Figure 4

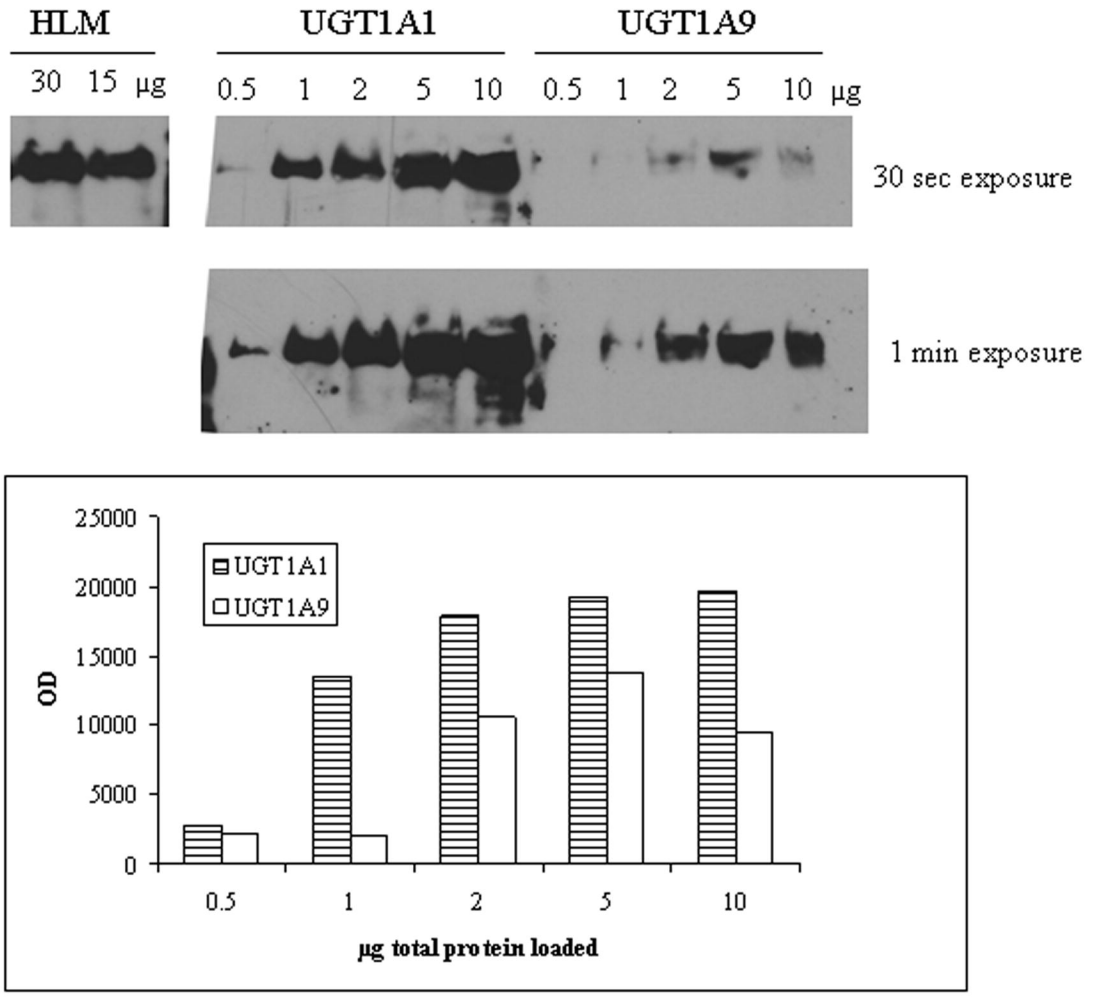

DMD Fast Forward. Published on November 8, 2007 as DOI: 10.1124/dmd.107.018788
This article has not been copyedited and formatted. The final version may differ from this version.

Figure 5

A)

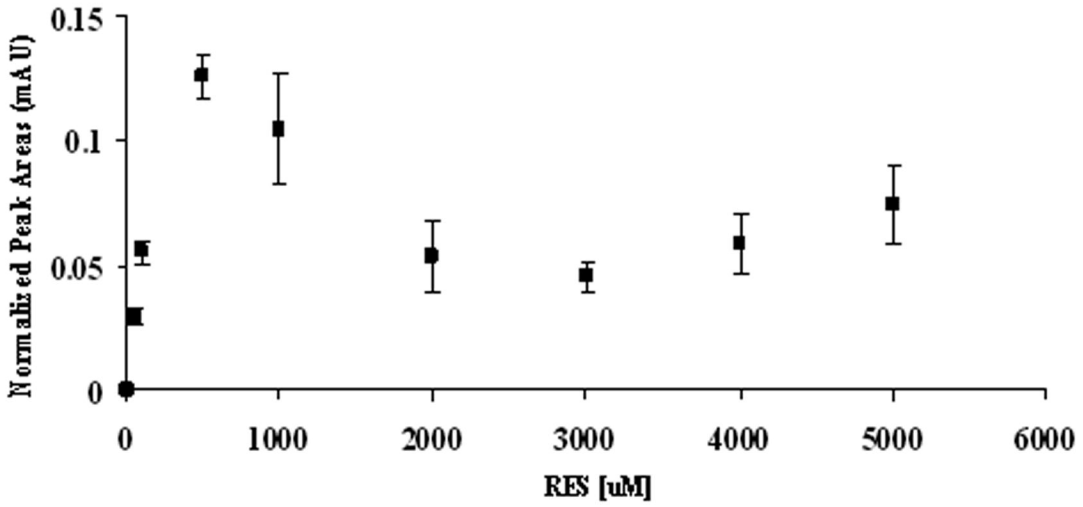

B)